Fingerprints of Delocalized Transition States in Quantum Dynamics

Hermann Frank von Horsten,[†] Guntram Rauhut,[‡] and Bernd Hartke*[,†]

Institut für Physikalische Chemie, Christian-Albrechts-Universität, Olshausenstrasse 40, 24098 Kiel, Germany, and Institut für Theoretische Chemie, Universität Stuttgart, Pfaffenwaldring 55, 70569 Stuttgart, Germany

Received: May 18, 2006; In Final Form: September 16, 2006

Reactions with delocalized transition states (plateau reactions) can be characterized statically by their energy profile along the reaction path, where they exhibit a broad, flat region instead of one or several well-defined saddle points on the potential energy surface. Employing our new, highly flexible quantum dynamics code to perform two-dimensional and effective four-dimensional quantum wave packet propagations on ab initio based model potentials, we show that plateau reactions can also be discerned from the other standard reaction types by their dynamics.

1. Introduction

Instead of a usual, i.e., localized, transition state, plateau reactions exhibit a flat region in their energy profile along the reaction path. This puts them between the textbook case of a simple barrier reaction (Eckart potential profile) and a two-step case with a reactive intermediate. First one-dimensional studies of plateau reactions have revealed that they show quite unusual features (vide infra) in contrast to standard concerted or stepwise mechanisms. At the moment, however, little is known about these reactions. Plateau reactions occur in different double proton transfer reactions (DPTRs) but also in other cases,[1−4] including biochemically relevant ones as the guanine/cytosine base pair.[5] Proton transfer steps not only are important for the currently frequently studied base pairs[6,7] but also often constitute key steps in chemical reaction mechanisms and biochemical processes.[8−12] Therefore it is important to investigate their dynamics in detail.

Single proton transfers have been intensely investigated, with high-level calculations and beyond the one-dimensional picture, leading to good agreement with experimental results.[13,14] Recently, even quantum effects on single proton-transfer steps in an enzymatic system have been studied.[15] In contrast, DPTR dynamics are much less well studied. Several groups have examined the formic acid dimer,[16−17] but due to symmetry this is a standard Eckart profile case, offering no insights for plateau reactions. Two of the present authors have studied DPTR plateau dynamics within the reaction path Hamiltonian (RPH) using classical mechanics,[19] showing that transition state theory is not applicable to these systems. The classical dynamics treatment within the RPH picture does not allow for a consistent investigation of the dynamical effects associated with the different potential energy surfaces when switching from a concerted to a stepwise reaction mechanism. In any case, the very light masses involved in DPTRs call for a quantum dynamical treatment. However, no higher-dimensional quantum mechanical dynamics studies of these systems are known to us, in fact not even one-dimensional ones.

Due to the size of the systems under consideration, the quantum dynamical treatment of these reactions will have to meet several challenges: (1) identification of the degrees of freedom (DOFs) most relevant to the reaction, (2) calculation of the potential energy surface in these degrees of freedom, to sufficient accuracy (presumably possible only on-the-fly), and (3) actually performing the quantum dynamics in all these degrees of freedom, which includes the problems of setting up the kinetic part of the Hamiltonian and of representing the multidimensional wave function.

Based on our exploratory studies using the RPH formalism, we expect that these systems will exhibit dynamical features that differ from both standard textbook cases of a single Eckart barrier and of a reactive intermediate. Therefore, it is crucial to characterize plateau dynamics in contrast to these two limiting cases.

Here, we present first steps toward quantum dynamics of plateau reactions, solving the challenge of setting up the kinetic part of the Hamiltonian. We work out first characteristic differences of this reaction type compared to the standard ones. To this end, we use both fully realistic ab initio quantum chemistry potentials and model potentials. The latter not only were initially fitted to these ab initio data but also offer the possibility to seamlessly switch between all three reaction types. All of these reaction types have already been detected by static energy profile analysis for pyrazole-guanidine clusters with varying substituent patterns.[4,20]

The remainder of this paper is organized as follows: In section 2 we briefly discuss relevant aspects of the theory. In section 3 we give essential details of our computational approach and of our test cases. In section 4 we present exemplary dynamical results for these systems. Section 5 finishes with a brief summary and conclusions.

2. Theoretical Background

All standard approaches to full quantum dynamics scale very steeply with the number of DOFs. To be able to focus the dynamical treatment on the internal DOFs of the molecule, one is therefore forced to abandon the simple form of the kinetic part of the Hamiltonian operator in Cartesian coordinates and to switch to curvilinear coordinates. However, this transforms the task of finding an analytical representation for the kinetic part of the Hamilton operator into a real problem.[21] Already for rather small systems, computer algebra programs have been

* Corresponding author. E-mail: hartke@phc.uni-kiel.de.
[†] Christian-Albrechts-Universität.
[‡] Universität Stuttgart.

10.1021/jp063051c CCC: $33.50
Published on Web 11/11/2006

employed for this task, resulting in long and complicated expressions that are awkward to handle.[22] Additionally, the resulting expressions (and computer programs) are not universal but have to be changed for each new case to be treated. If constraints need to be added, as in the case of limiting the dynamics to various active subsets of all DOFs (which is essentially unavoidable for larger systems), this approach can become completely impracticable. Active development is being done in this area,[23] but these basic problems of the traditional approach still persist.

In the following, we will briefly review the basic formulas needed in this context, where for the sake of simplicity we restrict ourselves to the case of zero total angular momentum ($J = 0$). A detailed treatment including the case $J > 0$ can be found in references 24 and 25.

Assuming that the configuration for an N-atomic molecule is appropriately described in terms of $3N - 6$ internal coordinates $\mathbf{q} = (q^1,..., q^{3N-6})^T$, the general expression of the kinetic energy operator can be written in a very compact form[24−27]

$$\hat{T}(\mathbf{q},\hat{\mathbf{p}}) = \frac{1}{2}\sum_{i,j=1}^{3N-6} \hat{p}_i^{\dagger} g^{ij}(\mathbf{q})\, \hat{p}_j \tag{2.1}$$

where $\hat{p}_i = -i\hbar\partial/\partial q^i$ are the conjugate momentum operators, $\hat{p}_i^{\dagger} = J^{-1}(\mathbf{q})\,\hat{p}_i\, J(\mathbf{q})$ are their adjoints, and g^{ij} are the contravariant components of the metric tensor. J denotes the Jacobian determinant of the transformation from Cartesian to curvilinear coordinates.

Expanding eq 2.1 leads to an expression for the kinetic energy operator which is much better suited for numerical calculations

$$\hat{T}(\mathbf{q},\partial_{\mathbf{q}}) = \sum_{i,j=1}^{3N-6} f_2^{ij}(\mathbf{q})\,\frac{\partial^2}{\partial q^i \partial q^j} + \sum_{i=1}^{3N-6} f_1^{i}(\mathbf{q})\,\frac{\partial}{\partial q^i} \tag{2.2}$$

with

$$f_2^{ij}(\mathbf{q}) = -\frac{\hbar^2}{2} g^{ij}(\mathbf{q}) \tag{2.3}$$

$$f_1^{i}(\mathbf{q}) = -\frac{\hbar^2}{2}\sum_{j=1}^{3N-6}\left[J^{-1}(\mathbf{q})\,\frac{\partial}{\partial q^j}\,J(\mathbf{q})\right] g^{ij}(\mathbf{q}) + \left[\frac{\partial}{\partial q^j}\, g^{ij}(\mathbf{q})\right] \tag{2.4}$$

It should be noted here that all the above equations are valid only if the standard Euclidean volume element $\mathrm{d}\tau = J(\mathbf{q})\mathrm{d}\mathbf{q}$ has been used to normalize the wave function. In case an arbitrary weighting function ρ is used (i.e. $\int \psi^*(\mathbf{q})\psi(\mathbf{q})\rho(\mathbf{q})\mathrm{d}\mathbf{q} = 1$), the kinetic energy operator in eq 2.1 has to be modified according to $\hat{T} \rightarrow \hat{T}^{\rho} = J^{-1/2}\rho^{1/2}\hat{T}J^{1/2}\rho^{-1/2}$. As a consequence, the substitution $J \rightarrow \rho$ is necessary in eq 2.4, and an additional purely multiplicative term V_{ep} appears in eq 2.2. The latter, being a function of the coordinates only, is often referred to as the extrapotential term.[24]

However, if the size of the system under investigation exceeds a number of four or maybe five atoms, and if traditional means of wave function representation are used (which imply exponential scaling of computational expense), some kind of reduced-dimensionality approach is clearly unavoidable. One general strategy is to divide the whole set of degrees of freedom into an active subset, which is treated explictly (and exactly), and an inactive/passive subset, where approximations and/or constraints are applied to reduce the overall work. Three commonly used ways of treating inactive coordinates are as follows:

1. The rigid-constraint model:[28,29] Within this approach, the passive coordinates are held fixed, e.g. at their equilibrium values. The big advantage concerning the quantum chemistry calculations is, of course, that the PES is needed only in the active coordinates and only in the form of single-point calculations. However, freezing the passive coordinates may allow for energetically unfavorable motions of the molecule. Furthermore, there are no unique and obvious choices at which values to fix the passive coordinates.

2. The adiabatically constrained or flexible model:[30] This approach consists of adjusting the variation of the passive coordinates to those of the few active ones by means of a restricted local potential minimization. On the quantum chemistry side, the local minimizations increase the computational burden (but not as far as in the next case). They do, however, provide a unique, well-defined choice of coordinate values for the passive coordinates. In general, these values of the passive coordinates are not constant but rather functions of active coordinates. This may or may not agree with the dynamic propensities of the system. Therefore, in some cases this model is known to produce rather large and unrealistic effective masses and extrapotential terms.[31]

3. The (harmonic) adiabatic approximation (H)ADA:[32−34] In the adiabatic approximation, the active and passive coordinates are treated very analogously to the slow nuclei and fast electrons in the Born−Oppenheimer approximation. The major disadvantage is that the full PES for all coordinates is needed. One possible way to circumvent this problem is to perform a quadratic (harmonic) approximation of the potential perpendicular to the active minimum energy path or domain. In this sense the HADA is closely related to the RPH formalism.

But whatever the nature of the constraints, all of the above considerations concerning the derivation of the kinetic energy operator become more involved. This applies even if analytical expressions for the unconstrained system are available.[28] The reason is simply that imposing constraints modifies the metric of the (unconstrained) configuration space and thus the Jacobian. Hence, as the above formulas show, the kinetic energy operator also changes.

3. Computational Details

For our current and future work on quantum dynamics of plateau DPTR reactions, we need an efficient route for testing different sets of active DOFs and for treating passive coordinates on different levels as described in the previous section. The importance of these choices has been nicely pointed out in the recent literature, for example by Luckhaus.[35] Instead of deriving analytical expressions for the kinetic energy operator, we have therefore decided to adopt an alternative approach of Lauvergnat et al.[36,37] They have shown that it is possible to calculate the coefficients needed in the general expression for the operator of the kinetic energy, eq 2.2, numerically (but exactly), as a function of the current geometry. This also allows for a comparatively simple restriction of the dynamics to arbitrary subsets of active DOFs. (For brevity, in the following text, we use the designation TNUM both for this approach and for its implementation as a computer subroutine by Lauvergnat et al.)

We have joined the TNUM program of Lauvergnat et al. with state-of-the-art quantum wave packet propagation technology already present in our group, including various basis, grid, and DVR representations of the vibrational wave function as well as the most important time propagation algorithms (split-operator, symplectic, short iterative Lanczos, Chebyshev). The resulting quantum dynamics program can be used unchanged

to perform quantum dynamics for quasi-arbitrary choices of coordinates and active/passive DOF subsets, including differing numbers of DOFs. Of course, since for the present study we employ traditional direct product bases, practical applications here are still limited to relatively few DOFs.

As a standard case for a plateau system we are employing here the pyrazol-guanidine cluster, for which one- and two-dimensional potential energy surfaces are available from prior ab initio quantum chemistry calculations.[19,38] Along the one-dimensional reaction path (with all other coordinates relaxed), this system exhibits an almost exactly flat plateau. With the two NH-distances as active coordinates (and again with all other coordinates relaxed), the plateau stretches in two dimensions but is slightly less pronounced than in the 1D picture. This indicates that the plateau is not just a 1D feature (a valley with a level floor but steep walls) but a multidimensional one. Naturally, however, it does depend on the choice and treatment of coordinates: With the passive coordinates fixed at their values at the (formal) transition state, the plateau gives way to a well with a depth of 5 kJ/mol. The choice of passive coordinate treatment is further discussed below.

We know from previous work[4,19] that more than two coordinates are significantly involved in the reaction path, including heavy-atom motions such as relative translation and angular motion of the two monomers (which parallels findings on similar systems in the literature[35,39,40]). At the present state of propagation technology, we therefore see little chance for a full investigation of the dynamics of this system, including all 48 degrees of freedom. Hence, we have resorted to fitting a two-dimensional model surface to the ab initio data, consisting of a flexible set of Gaussians and polynomial functions. Variations of the fitting parameters allow for all deformations of the model surface needed in this context.

In section 4, we present quantum dynamics on this model surface, for five selected cases: (1) The *normal plateau system*, which is the original fit of the model potential to the ab initio data. Since the other coordinates were relaxed in the ab initio calculation but are held fixed here, the dynamics on this potential corresponds to a hypothetical system exhibiting a realistic plateau in two active coordinates. (An example for the effects of geometry relaxation in the kinetic energy operator is presented in section 4.3.) (2) The *extended plateau system*, in which the model potential of case (1) has been modified such that the plateau is considerably broader, exaggerating its dynamical effects. This situation has been found and studied for the system fluoropyrazol-guanidine.[20] (3,4) Two *Eckart systems*, in which the plateau is replaced by a single Eckart-type barrier in two different ways. (5) The *reactive intermediate system*, where a well appears in place of the plateau. Figure 1 shows one-dimensional cuts along the minimum-energy paths for all five cases. As discussed in previous work,[4,19,20,41] these energy profile variations can be understood as arising from the presence of two single-barrier reaction steps which can occur simultaneously (Eckart cases (1) and (2)) or successively (case (5)). The plateau cases (1) and (2) arise between these two limiting cases.

It should be emphasized here that the model potentials for all cases (2)−(5) were generated from case (1) by applying the smallest possible amount of deformation, keeping all other features of the two-dimensional PES (in particular including those away from the reaction path) as close to the original ab initio form as possible. For this reason, these deformed potentials can be expected to be good models for real DPTR systems exhibiting these energy profile features.[4,19,20,41] For the same reason, however, the profiles classified as "Eckart" here do not

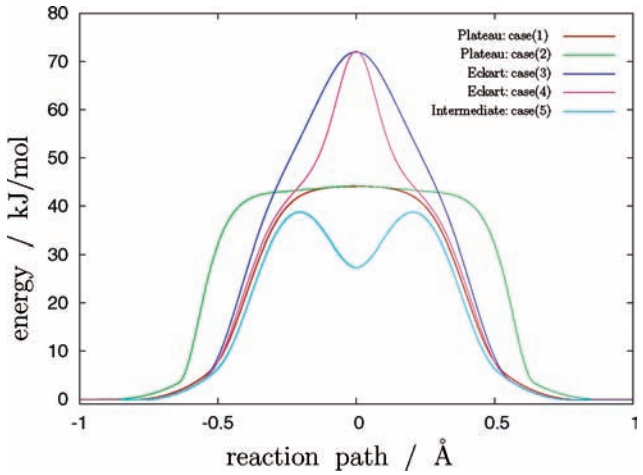

Figure 1. Energy profiles along the minimum-energy paths of the 5 model reaction types used here.

have pure Eckart form in the 1D cuts of Figure 1; in this sense, we use "Eckart" as a shorthand for a typical single barrier case. For simplicity, in the following we use the term "plateau region" not only just for the true plateau region of case (1) (corresponding to the reaction path interval [−0.25 Å, + 0.25 Å] in Figure 1) but also for the same spatial region in all other cases. In the present work, we are only interested in the dynamics in this plateau region; therefore, the form of the potentials beyond the reactant/product minima (outside of the reaction path interval depicted in Figure 1) is irrelevant to us and will be eliminated from the dynamics by absorbing potentials (see below).

These five prototype cases allow us to search for characteristic differences in the dynamical behavior of plateau reactions versus single and double Eckart barriers. One obvious candidate for marked differences in behavior is the residence time in the plateau region. Two of us have already investigated this quantity by approximate classical mechanical RPH dynamics.[19] From these studies, and from straightforward physical intuition, we expect it to be very small in cases (3,4) and large in case (5). However, it is a priori unclear whether a plateau system will be close to one of these two cases or between. As a simple but meaningful check for this situation we place an initial packet on the formal transition state, with a width on the order of the plateau width (case 1). To arrive at a meaningful comparison, we use the same initial wave packet $\psi(\cdot, t_0)$ for all cases, chosen to be a two-dimensional Gaussian

$$\psi(\mathbf{q}, t_0) = \prod_{j=1}^{2}\left(\frac{1}{\pi\sigma_j^2}\right)^{1/4} \exp\left(-\frac{(q^j - \tilde{q}^j)^2}{2\sigma_j^2}\right) \qquad (3.1)$$

centered at coordinates $\tilde{q}^j = 1.45$ Å and with widths $\sigma_j = 0.15/\sqrt{2}$ Å. Figure 2 depicts this initial wave packet on a two-dimensional view of the PES for case (1), in the NH-distances q^j ($j = 1, 2$).

It should be pointed out that this initial packet is not merely a technically helpful construction but simultaneously a proposal for future experiments: As pointed out in previous work,[38,41] the PES of certain excited states of plateau systems appear to be mirror images of the ground state PES, with a broad minimum in the region of the ground state plateau. Thus it appears possible that the initial state we are using here may actually be accessible to experimental preparation via suitably designed laser pump-dump schemes involving such an excited state.

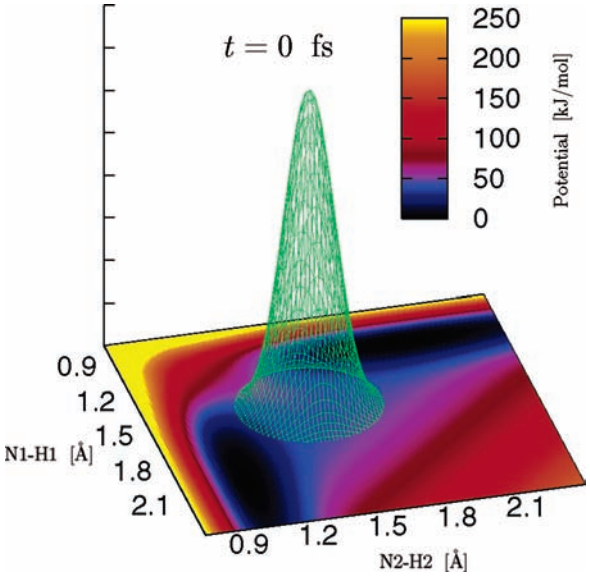

Figure 2. Initial wave packet in the plateau region of the 2D potential energy surface (case (1)). The potential is depicted with a color code (in kJ/mol). The two stretch coordinates are shown in Å.

As measures for the retention of the initial wave packet in the plateau region we employ the autocorrelation function and the quantum mechanical flux leaving the plateau area. The autocorrelation function $\mathcal{A}$ is defined as

$$\mathcal{A}(t) = \int \psi^*(\mathbf{q}, t_0)\, \psi(\mathbf{q}, t)\, \mathrm{d}\mathbf{q} \tag{3.2}$$

where we have used the Wilson normalization convention,[42,43] i.e., $\rho(\mathbf{q}) = 1 \Rightarrow \mathrm{d}\tau = \mathrm{d}\mathbf{q}$. Due to the specially chosen spatial extent and location of the initial packet, the absolute value of $\mathcal{A}$ already provides indications for the retention time of the packet in the plateau region. However, since $\psi(\mathbf{q}, t)$ and hence also $\mathcal{A}(t)$ are complex quantities in general, it is not strictly conclusive to examine $|\mathcal{A}(t)|$ (a single real function) alone. Or, in other words, a decrease in $|\mathcal{A}(t)|$ can be caused by decrease of overlap between $\psi(\mathbf{q}, t)$ and $\psi(\mathbf{q}, t_0)$ in coordinate space or in momentum space (or both).

In earlier cases,[44] we have also examined the phase of $\mathcal{A}(t)$ to overcome this ambiguity. Instead, in the present case of more complex dynamics, we additionally monitor the quantum mechanical flux leaving the reaction barrier region. For this purpose, we have defined this region as a simple square area $A \equiv \{\mathbf{q} \in \mathbb{R}^2 | \forall j \in \{1, 2\}: q^j \geq 1.2\ \text{Å} \wedge q^j \leq 1.7\ \text{Å}\}$. The flux through the boundaries ∂A of this area, denoted as $\mathcal{F}$, can then be written as

$$\mathcal{F}(t) = \oint_{\partial A} \mathbf{j}\cdot\mathbf{n}\, \mathrm{d}S = \int_A \nabla\cdot\mathbf{j}\, \mathrm{d}\mathbf{q}$$
$$\text{with} \quad \nabla\cdot\mathbf{j} = 2\hbar\, \mathrm{Im}(\psi(\mathbf{q}, t)\, \hat{T}\, \psi(\mathbf{q}, t)) \tag{3.3}$$

and the common notations for the flux density $\mathbf{j}$, the outward pointing unit normal $\mathbf{n}$ and the surface element $\mathrm{d}S$. We have tested different reasonable sizes and shapes for the area A, ensuring that the results are qualitatively independent of the special choice made in the current presentation.

The results presented in the following section are all obtained on a spatial grid between $q^j_{\min} = 0.6$ Å and $q^j_{\max} = 2.4$ Å, using 80 gridpoints per dimension. Convergence of the results is checked with higher numbers of gridpoints up to 100×100. For time propagation, we use the short iterative Lanzcos scheme[45] with dimension 12 for the Krylov subspace and a time step of 0.1 fs. Without the absorbing potential, deviations from energy conservation are then ensured to stay below 10^{-5} kJ/mol. For the absorbing potential $\mathcal{V}$, we apply the complex version of Manolopoulos[46] and Zhang[47]

$$\mathcal{V}(\mathbf{q}) = \sum_{j=1}^{2} V_{R,j} \exp(-\alpha_{R,j}\, \kappa_j) + iV_{I,j} \exp(-\alpha_{I,j}\, \kappa_j)$$
$$\text{with} \quad \kappa_j = \frac{q^j_{\max} - q^j}{q^j - q^j_0} \tag{3.4}$$

The starting coordinates of the absorbing potential are set to $q^j_0 = 2.15$ Å. The amplitudes of the real and imaginary part are $V_{R,j} = -0.127\, E_{\mathrm{t,max}}$ and $V_{I,j} = -0.994\, E_{\mathrm{t,max}}$, respectively. For the dimensionless parameters in the exponents we use $\alpha_{R,j} = 0.739$ and $\alpha_{I,j} = 3.071$. Under these conditions, we have verified that no parts of the wave packet reach the grid boundaries.

4. Results

4.1. Plateau vs Eckart. Figure 3 shows snapshots of the propagation of our initial packet on the plateau PES (case 1). A considerable amount of a surprisingly long-time retention of the wave packet in the (blue) plateau region is visible, but in this presentation this effect is obscured by other features of the evolving wave packet that are irrelevant for our purposes.

Since it is difficult to easily show the differences between the various cases in this form of presentation, we focus on more condensed but also clearer information in the following. Figure 4 shows the modulus of the autocorrelation functions for 2D quantum dynamics for the five test cases described in section 3. As explained there, due to the spatial extent of the initial packet, the autocorrelation function is a good measure for the retention time of the packet in the plateau region. The fluxes provide a complementary view and ensure that the autocorrelation data are not misinterpreted.

As expected, in the two Eckart cases (3) and (4), the autocorrelation falls off to almost zero without noticeable features within 5−10 fs, corresponding to a fast and essentially complete departure of the initial packet from the plateau region. This is confirmed by the strong initial flux peaks, followed by a quick return to the baseline. Apparently, the dynamical differences between the two Eckart cases are only minor. At about 30 fs, the wave packets have oscillated back and forth in the reactant/product minima (black regions in Figure 2) and partially return to the plateau region. To prevent this, we have applied absorbing potentials at the boundaries of the propagation grid. The remaining increase of the autocorrelation functions at about 30 fs is largely due to a partial revival based on oscillation in the symmetric stretch mode (along the bisectoring line). In any case, the dynamics beyond 30 fs is not dominated by the shape of the PES in the plateau region anymore. Therefore we focus the following discussion only on the initial time up to 30 fs.

The autocorrelation function for case (1) (corresponding to the original ab initio data of pyrazol-guanidine) strongly differs from both Eckart cases. Besides falling off more slowly, this initial falloff is only to a value of 0.2, indicating retention of a surprisingly large part of the wave packet on the plateau, which disappears only on a longer time scale. Correspondingly, the initial flux peak at 3 fs is much smaller than in both Eckart cases, and the following falloff to zero is less rapid and more structured.

This is again clearly different from case (5) (reactive intermediate). There, we find retention to a much higher level of 0.4 in the autocorrelation. As an additional signature of a

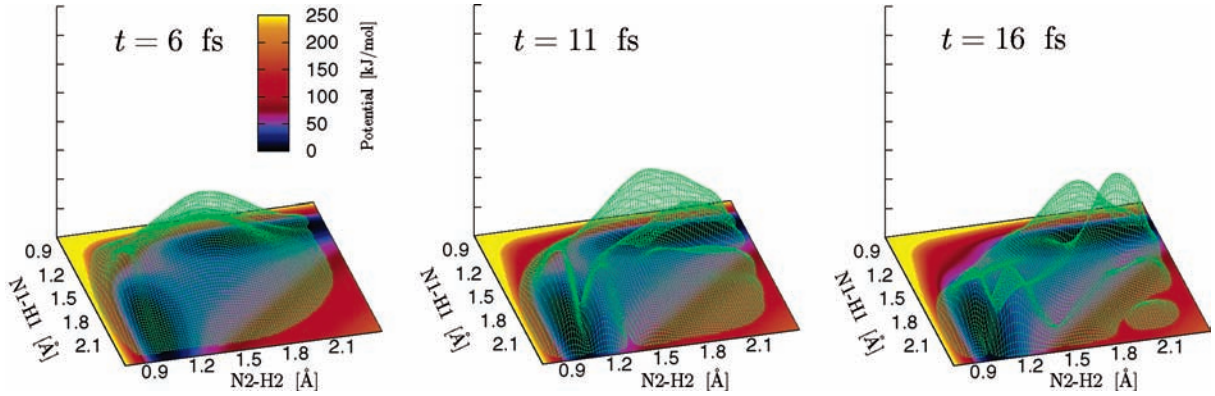

Figure 3. Propagating wave packet on the 2D plateau potential (case (1)). Presentation as in Figure 2.

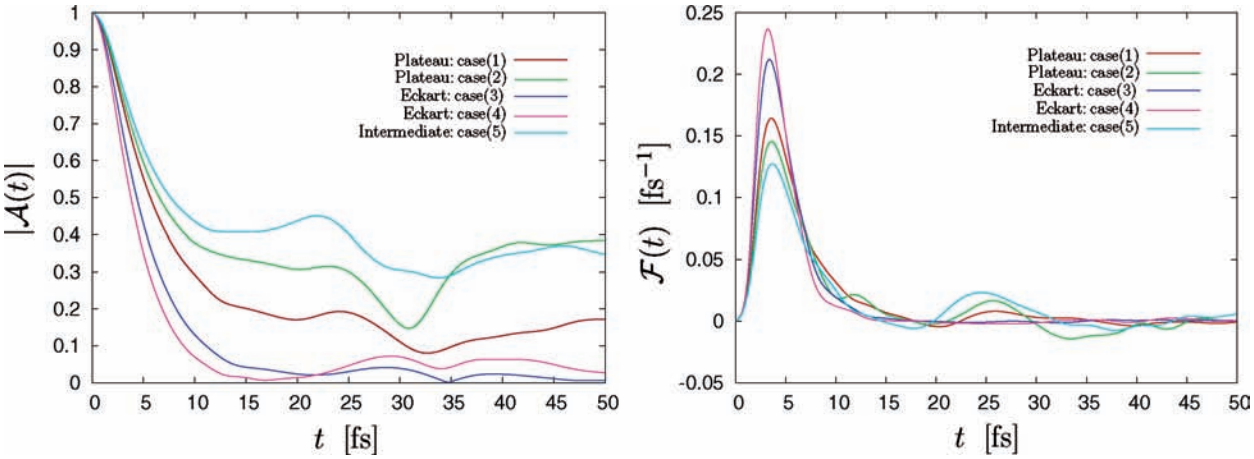

Figure 4. Absolute value of the autocorrelation functions (left-hand) and quantum mechanical fluxes (right-hand) for 2D dynamics of the 5 model reaction types used here plotted against the propagation time *t*.

potential well, two peaks of a vibrational movement in this well with a period of about 10 fs are visible (at 22 and 32 fs). Again, both features (higher retention and systematic oscillations) are also visible in the flux data.

This strong retention effect is induced by a comparatively small well (cf. Figure 1). Or, viewing the situation from a different perspective, getting the same amount of retention using a plateau without any well is surprisingly difficult. Of course, retention on a plateau increases if the plateau is extended. However, as case (2) shows, even if the length of the plateau along the reaction path is doubled, the retention effect is still clearly below that of the reactive intermediate case (5) (and discernible by the shape of the autocorrelation and flux data).

Therefore, plateau reactions are not just an elusive borderline phenomenon but presumably constitute a class of their own, distinct from the two textbook cases of a single Eckart barrier and of a reactive intermediate.

4.2. Quantum vs Classical Mechanics. The main aim of the present work is to show that plateau reactions form a class of their own, with distinctive features in their dynamics, as compared to single-barrier and reactive-intermediate situations, even in a quantum dynamical treatment, as it is appropriate for dynamics mainly dominated by light hydrogen atoms. This has been demonstrated by the result presented above. As additional aspect, one may ask if this special status of plateau reaction dynamics has quantum or classical mechanical origins. In our previous work,[19,20] we have already performed classical-mechanical dynamics, albeit for an RPH representation of these systems, which is not directly comparable to the models studied here. Therefore, we have also performed classical trajectory calculations for the present model cases.

Specifically, we have run large swarms of trajectories with initial conditions sampled from a Wigner quasi-probability distribution *W*, which for the initial wave packet (eq 3.1) is given by

$$W(\mathbf{q},\mathbf{p}) = \prod_{j,k} \frac{1}{\pi\hbar} \exp(-\sigma_j^{-2}(q^j - \tilde{q}^j)^2) \exp(-\sigma_k^{2}(p^k - \tilde{p}^k)^2) \tag{4.1}$$

The average values for the momenta $\tilde{p}^k$ are zero, and all other parameters are the same as described in section 3.

The classical Hamilton function *H* here reads

$$H(\mathbf{q},\mathbf{p}) = \frac{1}{2}\mathbf{p}\cdot\mathbf{g}(\mathbf{q})\cdot\mathbf{p} + V(\mathbf{q}) \tag{4.2}$$

where **g** is again the contravariant metric tensor from eq 2.1. To solve the canonical equations of motion

$$\dot{q}^j = \sum_k g^{jk}(\mathbf{q})\, p_k \tag{4.3}$$

and

$$\dot{p}^j = \frac{1}{2}\sum_{k,l} \frac{\partial g^{kl}(\mathbf{q})}{\partial q^j} p_k p_l - \frac{\partial V(\mathbf{q})}{\partial q^j} \tag{4.4}$$

We also need the derivatives of the **g** metric with respect to the active coordinates q^j. These are also easily computed with the TNUM code.

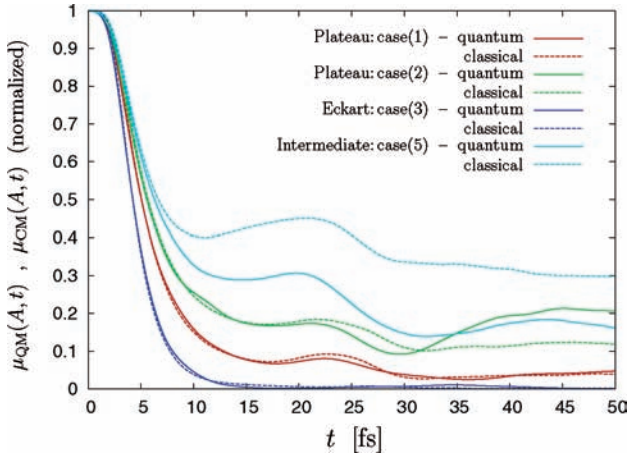

Figure 5. Quantum mechanical (solid lines) and classical (dashed lines) probability measures (normalized to one) for four of the test cases plotted against the propagation time t in femtoseconds.

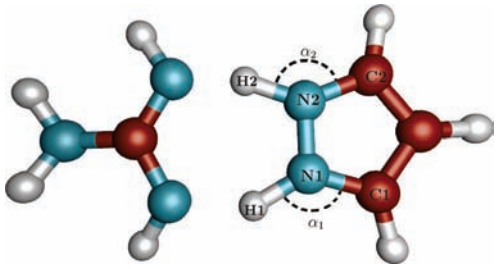

Figure 6. The two angular coordinates (α_1,α_2) incorporated into the dynamics via the flexible model.

For the classical time propagation we use a fourth-order Runge−Kutta algorithm with a time step of 0.1 fs. This ensures energy conservation to within 10^{-3} kJ/mol.

Figure 5 shows direct comparisons between the quantum mechanical and classical probability measures $\mu_{QM}(A, \cdot) = \int_A |\psi(\mathbf{q}, \cdot)|^2 \, d\mathbf{q}$ and $\mu_{CM}(A, \cdot) = \sum_{i=1}^{N_{ij}} \Theta_A(i, \cdot)$ as functions of the propagation time. Here, the function $\Theta_A(\cdot, t)$ counts the numbers of trajectories inside the spatial area A (the same area as the one described in section 4.1) at time t, where the total number of trajectories N_{ij} for each case is 215 760 sampled from eq 4.1. In order not to overload the figure we do not show the second Eckart case (case (4)) here, as the results are qualitatively the same as for case (3).

Obviously, the differences between classical and quantum mechanical dynamics are completely negligible for the Eckart case(s). Here, it is important to remember that we are using very special initial conditions ("on top of the barrier"), and therefore tunneling through the Eckart barrier is not expected to be an issue. Likewise, effects from vibrational zero-point energies are not expected to induce qualitative changes in dynamical behavior.

For the case (1) plateau, classical and quantum mechanics again are identical within the trajectory sampling error. As expected for a broader barrier, and as explicitly demonstrated in our previous work,[4] tunneling is unimportant for plateau cases, even for different initial conditions (corresponding to a full reaction, i.e., from one minimum over the barrier to the other minimum).

First differences between classical and quantum mechanics are visible for the still broader case (2) plateau, and they become significant for the case of a reactive intermediate. In the latter case, tunneling out of the shallow reactive intermediate well contributes to this effect. In both cases, however, also variations of vibrational zero-point energy along the reaction path have decisive effects. As we concluded in ref 20, this can transform shallow reactive intermediate wells into effective plateaus or even small effective barriers or vice versa. In fact, this conclusion was our main reason for switching from classical to quantum mechanical dynamics with the present work.

In summary, the presence of a plateaulike energy profile is also qualitatively discernible in a classical trajectory treatment. However, clear distinctions between true plateau cases and deviations from them toward small single or double barrier cases can only be made with a quantum dynamical treatment.

4.3. Rigid vs Flexible Model. As an example for the effects of incorporating geometry relaxation of inactive coordinates into the kinetic part of the Hamiltonian, we use the flexible model for the two angular coordinates $\alpha_i = \angle(H_i, N_i, C_i)$, depicted in Figure 6. From our previous studies,[19] we know that these two coordinates are among those with larger contributions to the reaction path. Numerical single-point information on the dependence of these two passive coordinates on the values of the two active stretch coordinates was extracted from the available ab initio data. Analytical fits of simple polynomials to these data enabled us to provide analytical derivatives of these dependencies, which is necessary input information for incorporation of these two DOFs as flexible passive ones into the numerical kinetic energy part of the Hamiltonian.

Figure 7 shows the autocorrelation functions and fluxes for this new case (using again the same initial wave packet), in direct comparison to the previously shown case (plateau case

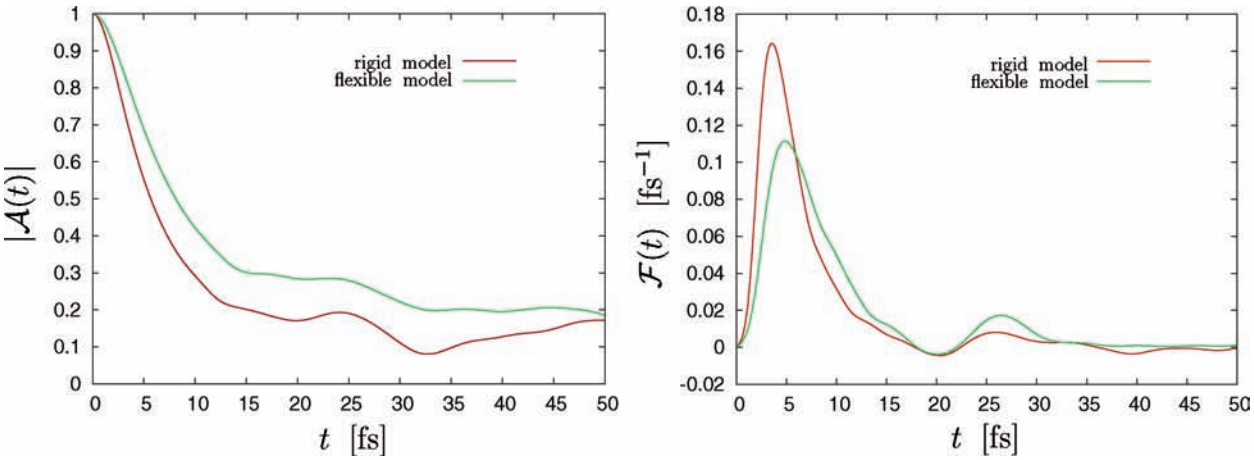

Figure 7. Absolute value of the autocorrelation functions (left-hand) and quantum mechanical fluxes (right-hand) for all passive coordinates taken as rigid (red lines), compared with two angular coordinates treated as flexible (green lines).

(1) in Figure 4) where these two passive coordinates were rigid (as all the other passive ones).

Clearly, the difference in the autocorrelation functions between these two ways of treating the passive coordinates in a plateau reaction is smaller than the differences for different reaction types (cf. Figure 4). They are also smaller than those observed for tunneling splittings in an Eckart-potential energy profile.[35] However, they clearly are far from negligible. An analysis of the corresponding wave packet movement (not shown) reveals that in the flexible case the effective 2D wave packet spreads more slowly (corresponding to a larger effective mass), in particular in the asymmetric stretch direction (perpendicular to the bisectoring line). This causes the higher retention effect visible in the autocorrelation function during the first 30 fs. This analysis is confirmed by the flux data, which exhibit a more significant difference.

Whether a rigid, a flexible or an (harmonic) adiabatic treatment is more appropriate for the inactive coordinates, and, even more importantly, how many and which coordinates should be active, depends on the dynamical propensities of the system under study. It has to be determined either a priori by educated guesses or a posteriori by investigating the convergence of dynamical properties upon increasing the number of active coordinates. Only an analysis of the dynamics in such a fully converged set of active coordinates will then reveal the true character of the reaction. This will then also be a more reliable indicator than the static, effective 1D picture of energy profiles along the reaction path given in Figure 1, which is biased by the particular definition of the reaction coordinate or by the desire to achieve a unique 1D cut in an electronic structure calculation.

For the present case of a plateau DPT reaction, our chemical intuition tells us that it is presumably correct to include the two angular DOFs as flexible passive coordinates, since the effective masses associated with them presumably are small enough to adapt to the proton movement. In contrast, we expect that this approach may be invalid for other dynamically important DOFs, for instance for those linked to relative translational movement of the whole pyrazole and guanidine fragments. An a posteriori confirmation of these hypotheses, however, can only be given after further method development toward quantum dynamcis for significantly more degrees of freedom.

5. Conclusions

We have linked state-of-the-art quantum wave packet propagation technology with a flexible numerical representation of the kinetic part of the Hamiltonian by Lauvergnat et al., establishing a first version of an all-purpose quantum dynamics program. Using available ab initio data on the paradigmatic DPTR plateau case of pyrazol-guanidine, we have constructed a 2D model potential energy surface that can be used as a tunable system, to seamlessly switch between various plateau types and the standard textbook cases of a single Eckart barrier and of a reactive intermediate. We have used these two ingredients to demonstrate special dynamical characteristics of plateau DPTR reactions, in contrast to those two standard textbook cases. It turns out that already simple measures such as retention times of a wave packet in the TS region allow for a differentiation between the dynamics of these three reaction types, putting them into three distinct classes.

Besides treating the passive degrees of freedom as rigid, we have also examined modeling them as flexible, which turns out to have visible influence on the dynamics without disrupting our reaction type classification. Ongoing work in our labs establishes higher-dimensional but sparse representations of vibrational wave packets[48] and system-specific global reoptimization of parameters in semiempirical methods.[49] Combination of these techniques with those presented here will allow for a quantum dynamical treatment of plateau DPTR reactions in all relevant degrees of freedom. This will be the topic of our future work.

Acknowledgment. F.v.H. and B.H. thank the group of Michèle Desouter-Lecomte (Paris-Sud), in particular David Lauvergnat and Benjamin Lasorne, for giving us their TNUM program and for helpful discussions regarding its use. Financial support for this work via DFG Grants RA 656/9-1 and HA 2498/6-1 is gratefully acknowledged.

References and Notes

(1) Gans-Eichler, T.; Gudat, D.; Nättinen, K.; Nieger, M. *Chem.—Eur. J.* **2006**, *12*, 1162.
(2) Li, P.; Bu, Y. *J. Phys. Chem. A* **2004**, *108*, 10288.
(3) Raynaud, C.; Daudey, J. P.; Maron, L.; Jolibois, F. *J. Phys. Chem. A* **2005**, *109*, 9646.
(4) Schweiger, S.; Rauhut, G. *J. Phys. Chem. A* **2003**, *107*, 9668.
(5) Guallar, V.; Douhal, A.; Moreno, M.; Lluch, J. *J. Phys. Chem. A* **1999**, *103*, 6251.
(6) Bertran, J.; Oliva, A.; Rodriguez-Santiago, L.; Sodupe, M. *J. Am. Chem. Soc.* **1998**, *120*, 8159.
(7) Sobolewski, A. L.; Domcke, W. *Phys. Chem. Chem. Phys.* **2004**, *6*, 2763.
(8) Caldin, E. F.; Gold, V. *Proton-Transfer Reactions*; Chapman and Hall: London, 1975.
(9) de la Vega, J. R.; Bisch, J. H.; Schauble, J. H.; Kunze, K. L.; Haggert, B. E. *J. Am. Chem. Soc.* **1982**, *104*, 3295.
(10) Meuwly, M. *Fut. Generations Comput. Systems* **2005**, *21*, 1285.
(11) Nir, E.; Kleinermanns, K.; de Vries, M. S. *Nature (London)* **2000**, *408*, 949.
(12) Shiau, W.-I.; Duesler, E. N.; Paul, I. C.; Curtin, D. Y.; Blann, W. G.; Fyfe, C. A. *J. Am. Chem. Soc.* **1980**, *102*, 4546.
(13) Matanovic, I.; Doslic, N. *J. Phys. Chem. A* **2005**, *109*, 4185.
(14) Yagi, K.; Taketsugu, T.; Hirao, K. *J. Chem. Phys.* **2001**, *115*, 10647.
(15) Wang, M.; Lu, Z.; Yang, W. *J. Chem. Phys.* **2006**, *124*, 124516.
(16) Markwick, P. R. L.; Doltsinis, N. L.; Marx, D. *J. Chem. Phys.* **2005**, *122*, 054112.
(17) Milnikov, G. V.; Kühn, O.; Nakamura, H. *J. Chem. Phys.* **2005**, *123*, 074308.
(18) Vener, M. V.; Kühn, O.; Bowman, J. M. *Chem. Phys. Lett.* **2001**, *349*, 562.
(19) Schweiger, S.; Hartke, B.; Rauhut, G. *Phys. Chem. Chem. Phys.* **2004**, *6*, 3341.
(20) Schweiger, S.; Hartke, B.; Rauhut, G. *Phys. Chem. Chem. Phys.* **2005**, *7*, 493.
(21) Meyer, H. *Annu. Rev. Phys. Chem.* **2002**, *53*, 141.
(22) Colwell, S. M.; Handy, N. C. *Mol. Phys.* **1997**, *92*, 317.
(23) Mladenović, M. *J. Chem. Phys.* **2000**, *112*, 1082.
(24) Chapuisat, X.; Belafhal, A.; Nauts, A. *J. Mol. Spectrosc.* **1991**, *149*, 274.
(25) Nauts, A.; Chapuisat, X. *Mol. Phys.* **1985**, *55*, 1287.
(26) Margenau, H.; Murphy, G. M. *The Mathematics of Physics and Chemistry;* Van Nostrand: Princeton, NJ, 1956.
(27) Podolsky, B. *Phys. Rev.* **1928**, *32*, 812.
(28) Chapuisat, X.; Nauts, A. *Mol. Phys.* **1997**, *91*, 47.
(29) Nauts, A.; Chapuisat, X. *Chem. Phys. Lett.* **1987**, *136*, 164.
(30) Gatti, F.; Justum, Y.; Menou, M.; Nauts, A.; Chapuisat, X. *J. Mol. Spectrosc.* **1997**, *181*, 403.
(31) Blasco, S. Ph.D. Thesis, Université de Paris-Sud, 2003.
(32) Blasco, S.; Lauvergnat, D. *Chem. Phys. Lett.* **2003**, *373*, 344.
(33) Lauvergnat, D.; Nauts, A. *Chem. Phys.* **2004**, *305*, 105.
(34) Lauvergnat, D.; Nauts, A.; Justum, Y.; Chapuisat, X. *J. Chem. Phys.* **2001**, *114*, 6592.
(35) Luckhaus, D. *J. Phys. Chem. A* **2006**, *110*, 3151.
(36) Lauvergnat, D.; Nauts, A. *J. Chem. Phys.* **2002**, *116*, 8560.
(37) Lauvergnat, D.; Baloïtcha, E.; Dive, G.; Desouter-Lecomte, M. *Chem. Phys.* **2006**, *326*, 500.
(38) Rauhut, G.; Schweiger, S. In *High Performance Computing in Science and Engenieering '04*; Krause, E., Jäger, W., Resch, M., Eds.; Springer: Berlin, Heidelberg, 2005; p 323.
(39) Benderskii, V.; Makarov, D.; Wright, C. *Adv. Chem. Phys.* **1994**, *88*, 179.
(40) Shida, N.; Barbara, P.; Almlof, J. *J. Chem. Phys.* **1991**, *94*, 3633.

(41) Schweiger, S.; Rauhut, G. *J. Phys. Chem. A* **2006**, *110*, 2816.
(42) Wilson, E. B., Jr.; Decius, J. C.; Cross, P. C. *Molecular Vibrations;* McGraw-Hill: New York, 1955.
(43) Chapuisat, X.; Nauts, A.; Brunet, J. P. *Mol. Phys.* **1991**, *72*, 1.
(44) Skouteris, D.; Hartke, B.; Werner, H.-J. *J. Phys. Chem. A* **2001**, *105*, 2458.
(45) Park, T. J.; Light, J. C. *J. Chem. Phys.* **1986**, *85*, 5870.
(46) Manolopoulos, D. Charles Coulson summer school in theoretical chemistry, 1996.
(47) Ge, J.-Y.; Zhang, J. Z. H. *J. Chem. Phys.* **1998**, *108*, 1429.
(48) Hartke, B. *Phys. Chem. Chem. Phys.* **2006**, *8*, 3627.
(49) Palangsuntikul, R. Ph.D. Thesis, University of Kiel, 2005.